# Syntheses and Magnetic Properties of Imidazolate-Bridged Binuclear Copper(II) Complexes: Effect of Bridging Mode upon Magnetic Interaction

Sakurako Ohkubo, Keiji Inoue, Hiroko Tamaki, Masaaki Ohba, Naohide Matsumoto,* Hisashi Ōkawa, and Sigeo Kida†
Department of Chemistry, Faculty of Science, Kyushu University, Hakozaki, Higashi-ku, Fukuoka 812
†Kumamoto Institute of Technology, Ikeda 4-22-1, Kumamoto 860
(Received February 3, 1992)

Three imidazolate-bridged binuclear copper(II) complexes $[Cu(A)Cu(L^n)]ClO_4$, **1** ($n$=1), **2** ($n$=2), and **3** ($n$=3), have been prepared and characterized, where $H_2A$=4-(6-methyl-8-hydroxy-2,5-diazanonane-1,5,7-trienyl)-imidazole, $HL^1$=*N*-salicylidene-2-(2-pyridyl)ethylamine, $HL^2$=*N*-(1-methyl-3-oxobutylidene)-2-(2-pyridyl)ethylamine, and $HL^3$=3,3′-(trimethylenedinitrilo)-bis[2-butanone oximate]. The cryo-magnetic susceptibility data (4.2—300 K) of **1** and **2** were well reproduced by the Bleaney-Bowers equation based on $H=-2JS_{Cu}\cdot S_{Cu}$ with the $J$ values of −46.1 and −36.6 $cm^{-1}$, respectively, while the magnetic data of **3** showed no magnetic interaction. The reference complexes $[Cu(L^n)(py)]ClO_4$ ($n$=1,2; py=pyridine) have been subjected to single-crystal X-ray diffraction analysis.

The elucidation of the structural and electronic factors governing magnetic interaction between paramagnetic centers is of current interests.[1,2] Studies on hetero-metal polynuclear complexes are essentially important to elucidate the magnetic interaction between the magnetic centers exhibiting the distinct electronic configurations.[1-8] On the other hand, studies on homo-metal polynuclear complexes with dissimilar coordination geometries or with various bridging mode are also informative to understand the mechanism of magnetic interaction.[9-11] From the latter point of view, in this study three imidazolate-bridged binuclear copper(II) complexes $[Cu(A)Cu(L^n)]ClO_4$, **1** ($n$=1), **2** ($n$=2), and **3** ($n$=3), have been prepared and the magnetic properties have been investigated, where $H_2A$=4-(6-methyl-8-hydroxy-2,5-diazanonane-1,5,7-trienyl)-imidazole, $HL^1$=*N*-salicylidene-2-(2-pyridyl)ethylamine, and $HL^2$=*N*-(1-methyl-3-oxobutylidene)-2-(2-pyridyl)-ethylamine, and $HL^3$=3,3′-(trimethylenedinitrilo)-bis[2-butanone oximate]. Their schematic structures are shown in Fig. 1. In the binuclear complexes the [Cu(A)] moiety acts as a ligand and occupies an equatorial coordination site of $Cu(L^n)$ in the cases of **1** and **2**, whereas [Cu(A)] occupies an axial site in the case of **3**. In this study, the structural effects upon magnetic interaction are examined.

## Experimental

**Syntheses.** A component complex $[Cu(A)]\cdot 0.5CHCl_3$ ($H_2A$=4-(6-methyl-8-hydroxy-2,5-diazanonane-1,5,7-trienyl)-imidazole) was prepared by the method reported earlier.[9] The other component complexes $[Cu(L^n)H_2O]ClO_4$ ($n$=1, 2) ($HL^1$=*N*-salicylidene-2-(2-pyridyl)ethylamine, $HL^2$=*N*-(1-methyl-3-oxobutylidene)-2-(2-pyridyl)ethylamine), were obtained as green crystals by the reaction of copper(II) acetate monohydrate, $HL^n$, triethylamine, and $NaClO_4$ in methanol with the mole ratio of 1 : 1 : 1 : 1 according to the method of literature.[12] The component complex $[Cu(L^3)]ClO_4\cdot H_2O$ ($HL^3$=3,3′-(trimethylenedinitrilo)-bis[2-butanone oximate]) was prepared by the method of Gagne.[13] The reference complexes $[Cu(L^n)$(*N*-MeIm or py)$]ClO_4$ (*N*-MeIm=1-methyl-1*H*-imidazole, py=pyridine) were prepared by mixing $[Cu(L^n)H_2O]ClO_4$ and excess *N*-MeIm or py in methanol.

**$[Cu(A)Cu(L^1)]ClO_4$ (1).** To an acetone solution (30 $cm^3$) of $[Cu(L^1)H_2O]ClO_4$ (424 mg, 1 mmol) was added an acetone solution (50 $cm^3$) of $[Cu(A)]\cdot 0.5CHCl_3$ (341 mg, 1 mmol) at room temperature. The resultant dark brown solution was filtered and the filtrate was kept for several hours to precipitate dark violet microcrystals. They were collected by suction filtration and dried in air. Anal. Found: C, 44.93; H, 4.13; N, 12.40; Cu, 18.97%. Calcd for $C_{25}H_{27}ClCu_2N_6O_6$: C, 44.81; H, 4.06; N, 12.54; Cu, 18.66%. $\Lambda_M$(methanol) 118 S $mol^{-1}$ $cm^2$. The complexes $[Cu(A)Cu(L^2)]ClO_4$ (**2**) and $[Cu(A)Cu(L^3)]ClO_4$ (**3**) were prepared in a way similar to that

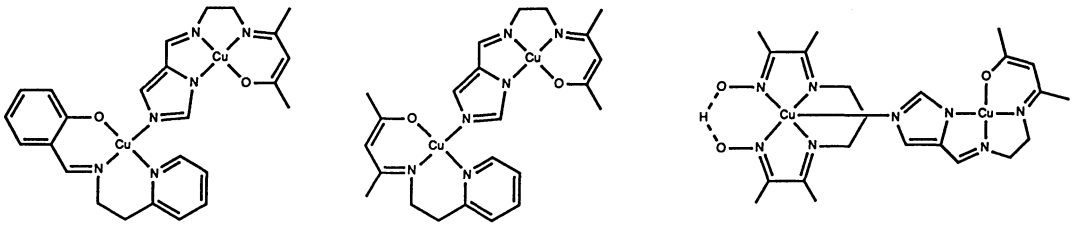

**1** **2** **3**

Fig. 1. Schematic structures of $[Cu(A)Cu(L^n)]^+$ **1**($L^1$), **2**($L^2$), and **3**($L^3$).

of **1**.

**[Cu(A)Cu(L²)]ClO₄·0.5H₂O (2).** Violet microcrystrals, Anal. Found: C, 42.18; H, 4.60; N, 12.53; Cu, 19.17%. Calcd for $C_{23}H_{30}ClCu_2N_6O_{6.5}$: C, 42.06; H, 4.60; N, 12.79; Cu, 19.34%. $\Lambda_M$(methanol) 112 S mol$^{-1}$ cm$^2$.

**[Cu(A)Cu(L³)]ClO₄·H₂O (3).** Violet microcrystals, Anal. Found: C, 37.34; H, 4.88; N, 15.67; Cu, 18.25%. Calcd for $C_{22}H_{35}ClCu_2N_8O_8$: C, 37.64; H, 5.03; N, 15.96; Cu, 18.10%. $\Lambda_M$(methanol) 143 S mol$^{-1}$ cm$^2$.

**Physical Measurements.** Elemental analyses for C, H, and N were performed at the Elemental Analysis Service Center of Kyushu University. Copper analyses were made on a Shimadzu AA-680 Atomic Absorption/Flame Emission Spectrophotometer. Infrared spectra were measured on KBr disks with a JASCO IR-810 spectrophotometer. Electrical conductivity measurements were carried out on a Denki Kagaku Keiki AOL-10 digital conductometer in ca. $10^{-3}$ mol dm$^{-3}$ solutions. Electronic spectra were measured on a Shimadzu MPS-2000 Multipurpose Recording Spectrophotometer. ESR spectra(X-band) were recorded on a JES-FE3X spectrometer. Magnetic susceptibilities were measured by the use of a HOXAN HSM-D SQUID susceptometer in the temperature range 4.2—100 K and by the use of a Faraday balance in the temperature range 80—300 K. The apparatus were calibrated with $Mn(NH_4)_2(SO_4)_2\cdot 6H_2O$ for SQUID susceptometer and with $[Ni(en)_3]S_2O_3$ for Faraday method. Diamagnetic corrections were made with Pascal's constants.[14] Effective magnetic moments were calculated by the equation $\mu_{eff}=2.828(\chi_A T)^{1/2}$, where $\chi_A$ is magnetic susceptibility per copper.

**X-Ray Structural Analysis.** X-Ray data were collected on a Rigaku Denki AFC-5 four-circle automated diffractometer with graphite-monochromatized Mo $K\alpha$ radiation at ambient temperature. The unit cell parameters were determined by 25 reflections in the range of $20°<2\theta<30°$. Standard reflections were monitored every 100 reflections and showed good stabilities. Intensity data were corrected for Lorentz and polarization effects but no absorption correction was applied. The details of data collection, crystallographic data, and data reduction are summarized as follows:

**[Cu(L¹)(py)]ClO₄.** Formula=$CuClO_5N_3C_{19}H_{18}$, formula weight=467.37, triclinic, space group=$P\bar{1}$, $a$=9.860(3), $b$=10.816(3), $c$=10.186(3) Å, $\alpha$=111.17(2), $\beta$=107.89(2), $\gamma$=78.02(2)°, $V$=958.3(5) Å$^3$, $Z$=2, $D_x$=1.619 g cm$^{-3}$, crystal dimensions 0.4×0.4×0.3 mm, $\mu$(Mo $K\alpha$) 12.882 cm$^{-1}$, octant measured $+h$, $+k$, $\pm l$, scan speed 4° min$^{-1}$, scan width (1.2+0.35 tan $\theta$)°, number of observed reflections with $|F_o|>3\sigma(|F_o|)$ 3783, $R$=3.55%, $R_w$=3.71%, weighting scheme $w$=1 for all reflections, largest residual peak 0.9 e Å$^{-3}$.

**[Cu(L²)(py)]ClO₄.** Formula=$CuClO_5N_3C_{17}H_{20}$, formula weight=445.36, monoclinic, space group=$P2_1/n$, $a$=14.357(2), $b$=14.990(4), $c$=9.191(1) Å, $\beta$=96.01(2)°, $V$=1953.9(6) Å$^3$, $Z$=4, $D_x$=1.514 g cm$^{-3}$, crystal dimensions 0.4×0.3×0.3 mm, octant measured $+h$, $\pm k$, $\pm l$, scan speed 4° min$^{-1}$, scan width (1.2+0.35 tan $\theta$)°, number of observed reflections with $|F_o|>3\sigma(|F_o|)$ 2803, $R$=7.19%, $R_w$=7.86%, weighting scheme

Table 1. Positional Parameters (×10$^{-4}$) of [Cu(L¹)(py)]ClO₄

| Atom | $x$ | $y$ | $z$ | $B_{eq}$[a)] |
|---|---|---|---|---|
| Cu | −1709.4(4) | 1051.0(3) | 171.6(4) | 2.5 |
| O1 | −664(2) | 81(2) | 1482(2) | 3.0 |
| N1 | −2950(3) | −387(2) | −958(2) | 2.6 |
| N2 | −2836(3) | 2114(2) | −1171(2) | 2.6 |
| N3 | −334(3) | 2469(2) | 1295(2) | 2.5 |
| C1 | −1230(3) | −685(3) | 1867(3) | 2.6 |
| C2 | −491(4) | −1051(3) | 3119(3) | 3.5 |
| C3 | −1016(4) | −1889(4) | 3526(4) | 4.5 |
| C4 | −2314(5) | −2413(4) | 2736(4) | 4.7 |
| C5 | −3048(4) | −2087(4) | 1509(4) | 3.9 |
| C6 | −2529(3) | −1244(3) | 1043(3) | 2.8 |
| C7 | −3239(3) | −1135(3) | −377(3) | 2.8 |
| C8 | −3696(3) | −582(3) | −2502(3) | 3.1 |
| C9 | −2930(3) | 32(3) | −3160(3) | 3.1 |
| C10 | −3212(3) | 1517(3) | −2629(3) | 2.7 |
| C11 | −3897(4) | 2249(3) | −3552(3) | 3.4 |
| C12 | −4265(4) | 3593(3) | −3008(4) | 3.7 |
| C13 | −3934(4) | 4192(3) | −1516(4) | 3.5 |
| C14 | −3218(3) | 3434(3) | −637(3) | 2.9 |
| C15 | 112(3) | 3145(3) | 662(3) | 2.9 |
| C16 | 1015(4) | 4124(3) | 1438(4) | 4.0 |
| C17 | 1483(4) | 4424(4) | 2926(4) | 4.6 |
| C18 | 1035(4) | 3749(3) | 3592(3) | 3.9 |
| C19 | 129(3) | 2776(3) | 2751(3) | 3.1 |
| Cl | −3388(1) | 3108(1) | 3138(1) | 2.9 |
| O2 | −4782(3) | 3428(2) | 3423(3) | 4.1 |
| O3 | −3509(3) | 2212(2) | 1674(2) | 4.2 |
| O4 | −2867(3) | 4292(2) | 3241(3) | 5.1 |
| O5 | −2411(3) | 2505(3) | 4132(3) | 5.9 |

a) $B$ values for anisotropic refined atoms are given in the form of the isotropic equivalent displacement parameters defined as $(4/3)[a^2B_{11}+b^2B_{22}+c^2B_{33}+ab\cos\gamma B_{12}+ac\cos\beta B_{13}+bc\cos\alpha B_{23}]$.

Table 2. Positional Parameters (×10$^{-4}$) of [Cu(L²)(py)]ClO₄

| Atom | $x$ | $y$ | $z$ | $B_{eq}$[a)] |
|---|---|---|---|---|
| Cu | 323(1) | 1611(1) | 949(1) | 3.3 |
| O1 | −186(4) | 897(4) | 2365(6) | 4.2 |
| N1 | −584(4) | 1238(4) | −663(6) | 3.5 |
| N2 | 706(4) | 2699(4) | −126(6) | 3.4 |
| N3 | 1518(4) | 1678(4) | 2317(6) | 3.4 |
| C1 | −1373(6) | 321(7) | 3634(10) | 5.6 |
| C2 | −1051(6) | 642(5) | 2225(9) | 4.3 |
| C3 | −1630(6) | 629(6) | 925(10) | 4.8 |
| C4 | −1385(6) | 901(5) | −442(9) | 4.2 |
| C5 | −2118(7) | 756(6) | −1712(12) | 6.5 |
| C6 | −392(6) | 1406(5) | −2144(9) | 4.8 |
| C7 | 590(6) | 1759(6) | −2256(8) | 4.8 |
| C8 | 739(5) | 2671(6) | −1565(8) | 3.9 |
| C9 | 886(6) | 3449(7) | −2342(10) | 5.4 |
| C10 | 1024(6) | 4238(6) | −1623(11) | 6.1 |
| C11 | 1010(6) | 4257(6) | −125(11) | 5.5 |
| C12 | 854(5) | 3477(6) | 585(9) | 4.4 |
| C13 | 2332(5) | 1566(5) | 1787(8) | 3.7 |
| C14 | 3164(5) | 1547(6) | 2674(9) | 4.3 |
| C15 | 3165(6) | 1685(6) | 4143(9) | 4.6 |
| C16 | 2322(6) | 1828(6) | 4705(8) | 4.9 |
| C17 | 1504(5) | 1812(6) | 3756(8) | 4.4 |
| Cl | 3909(2) | 1847(2) | −1340(2) | 6.0 |
| O2 | 4253(5) | 2061(6) | −2639(7) | 8.8 |
| O3 | 4253(7) | 2359(6) | −231(8) | 11.1 |
| O4 | 3535(9) | 1078(7) | −1168(14) | 17.1 |
| O5 | 2969(9) | 2268(12) | −1486(15) | 20.1 |

a) $B$ values for anisotropic refined atoms are given in the form of the isotropic equivalent displacement parameters defined as $(4/3)[a^2B_{11}+b^2B_{22}+c^2B_{33}+ab\cos\gamma B_{12}+ac\cos\beta B_{13}+bc\cos\alpha B_{23}]$.

$w=1/\sigma(|F_o|)$, largest residual peak 0.3 e Å$^{-3}$.

The structures were solved by the standard heavy-atom method and refined by the block-diagonal least-squares method. Reliability factors were defined as $R=\sum||F_o|-|F_c||/\sum|F_o|$ and the function minimized is $R_w=[\sum w(|F_o|-|F_c|)^2/\sum w|F_o|^2]^{1/2}$. Atomic scattering factors were taken from the literature.[15] The hydrogen atoms were inserted at the calculated positions and refined with the isotropic thermal parameters. Final difference Fourier syntheses were featureless. The computation was carried out on a FACOM V-100 computer at the Computer Center of Kyushu University using the UNICS III program system.[16] Tables of observed and calculated structure factors, atomic parameters of hydrogen atoms, anisotropic thermal parameters, and bond distances and angles are deposited as Document No. 9005 at the Office of the Editor of Bull. Chem. Soc. Jpn. Positional parameters of the non-hydrogen atms of $[Cu(L^1)(py)]ClO_4$ and $[Cu(L^2)(py)]ClO_4$ are given in Tables 1 and 2, respectively.

## Results and Discussion

The elemental analyses are consistent with the chemical formula of $[Cu(A)Cu(L^n)]ClO_4$ ($n$=1, 2, 3). The molar electrical conductivities of **1**, **2**, and **3** are 118, 112, and 143 S mol$^{-1}$ cm$^2$ in methanol, respectively, which fall in the range expected for 1 : 1 electrolyte. The infrared spectra of **1**, **2**, and **3** showed an intense broad band around 1100 cm$^{-1}$ due to perchlorate ion as non-coordinating counter anion. Imidazolate-bridged structures of **1**—**3** can be reduced by electronic spectral data of **1**—**3** and their component and reference complexes. The electronic spectrum of imidazole-bridged binuclear complexes $[Cu(A)Cu(L^n)]ClO_4$ is roughly consistent with the spectrum which superimposes the spectrum of the corresponding reference complex $[Cu(N\text{-MeIm})(L^n)]ClO_4$ on that of [Cu(A)]. The electronic spectra were deposited as supplementary data. The X-ray analyses of **1**, **2**, and **3** have not been successful yet, because these complexes were obtained as microcrystals but easily effloresced in open atmosphere. In order to estimate the structures, the reference complexes $[Cu(L^n)(py)]ClO_4$ ($n$=1, 2) have been subjected to single-crystal X-ray analyses.

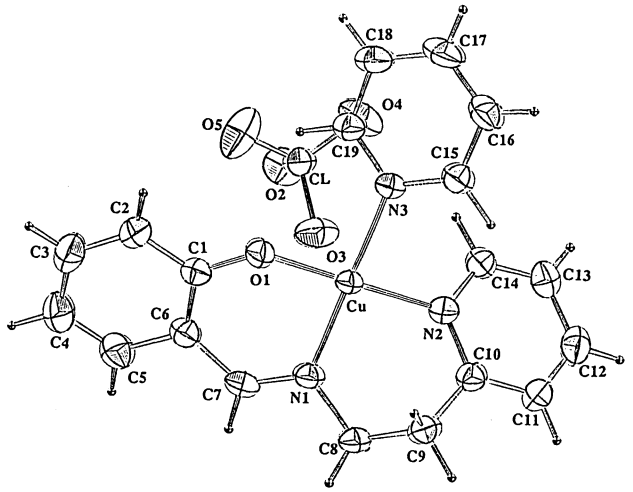


Fig. 2. ORTEP drawing of $[Cu(L^1)(py)]ClO_4$ with the atom numbering scheme, where the thermal ellipsoids for non-hydrogen atoms are drawn at 50% probability level.

**Structural Descriptions of Reference Complexes $[Cu(L^1)(py)]ClO_4$ and $[Cu(L^2)(py)]ClO_4$.** The ORTEP drawings of $[Cu(L^1)(py)]ClO_4$ and $[Cu(L^2)(py)]ClO_4$ with the atom numbering schemes are shown in Figs. 2

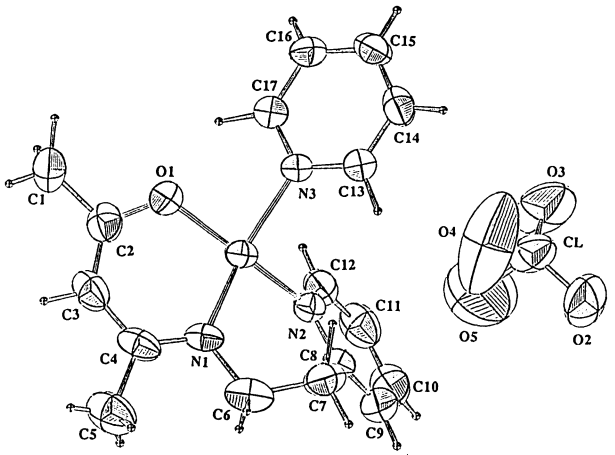


Fig. 3. ORTEP drawing of $[Cu(L^2)(py)]ClO_4$ with the atom numbering scheme, where the thermal ellipsoids for non-hydrogen atoms are drawn at 50% probability level.

Table 3. Selected Bond Distances and Angles of $[Cu(L^1)(py)]ClO_4$

| | | | |
|---|---|---|---|
| (a) Bond distances(Å) | | | |
| Cu–O1 | 1.914(2) | Cu–N1 | 1.968(3) |
| Cu–N2 | 2.025(3) | Cu–N3 | 2.035(3) |
| O1–C1 | 1.309(4) | N1–C7 | 1.277(4) |
| N1–C8 | 1.474(4) | N2–C10 | 1.352(4) |
| N3–C19 | 1.345(4) | | |
| (b) Bond angles(deg) | | | |
| O1–Cu–N1 | 90.8(1) | O1–Cu–N2 | 178.5(1) |
| O1–Cu–N3 | 78.1(1) | N1–Cu–N2 | 89.8(1) |
| N1–Cu–N3 | 176.8(1) | N2–Cu–N3 | 91.3(1) |

Table 4. Selected Bond Distances and Angles of $[Cu(L^2)(py)]ClO_4$

| | | | |
|---|---|---|---|
| (a) Bond distances(Å) | | | |
| Cu–O1 | 1.890(6) | Cu–N1 | 1.941(6) |
| Cu–N2 | 2.008(6) | Cu–N3 | 2.013(6) |
| O1–C2 | 1.29(1) | N1–C4 | 1.290(1) |
| N1–C6 | 1.44(1) | N2–C8 | 1.33(1) |
| N2–C12 | 1.34(1) | N3–C13 | 1.33(1) |
| N3–C17 | 1.34(1) | | |
| (b) Bond angles(deg) | | | |
| O1–Cu–N1 | 95.0(3) | O1–Cu–N2 | 160.3(3) |
| O1–Cu–N3 | 88.1(3) | N1–Cu–N2 | 93.1(3) |
| N1–Cu–N3 | 160.6(3) | N2–Cu–N3 | 90.3(3) |

and 3, respectively. Relevant interatomic bond distances and angles of $[Cu(L^1)(py)]ClO_4$ and $[Cu(L^2)(py)]ClO_4$ are given in Tables 3 and 4, respectively.

The copper(II) ion of $[Cu(L^1)(py)]ClO_4$ is coordinated by $N_2O$ donor atoms of tridentate ligand $L^1$ and a nitrogen atom of pyridine with the Cu–O, N bond distances of 1.914(3)—2.035(3) Å. As anticipated by the infrared spectrum, the oxygen atoms of perchlorate ion do not participate in coordination to copper(II) ion. The coordination geometry is described as a four-coordinated square planar geometry with a slight tetrahedral distortion, the atom deviations of O1, N1, N2, and N3 from the best-plane defined by coordinating $N_3O$ doner atoms being −0.04, +0.04, −0.04, and +0.04 Å, respectively. The pyridine plane is tilted to the coordination plane by 37.8° due to the steric hindrance from the pyridine moiety of the tridentate ligand.

The structural feature of $[Cu(L^2)(py)]ClO_4$ is essentially similar to that of $[Cu(L^1)(py)]ClO_4$. As shown in Fig. 4, tetrahedral distortion is enhanced in this complex and the coordination geometry can be described as an intermediate between square plane and tetrahedron. The atom deviations of O1, N1, N2, and N3 from the best-plane defined by $N_3O$ are +0.34, −0.32, +0.32, and −0.34 Å, respectively. The dihedral angle between CuO1N1 and CuN2N3 is 26.7°. The Cu–N, –O bond distances fall in the range 1.890(6)—2.013(6) Å. The pyridine plane is tilted to the coordination plane by 55.9° due to the steric hindrance from the pyridine moiety of the tridentate ligand, where the dihedral angle between the pyridine molecule and the pyridine moiety of tridentate ligand is 95.4°.

On the basis of the structures of the reference complexes, it is plausible that in **1** and **2** the imidazolate nitrogen atom of [Cu(A)] coordinates to $[Cu(L^n)]$ ($n$=1, 2) as one of the four equatrial atoms. On the other hand, it is expected that in **3** the nitrogen atom of [Cu(A)] occupies an axial site of $Cu(L^3)$. The crystal structure of $[Cu(L^3)(py)]ClO_4$ showed that the coordination geometry is a tetragonal pyramid with Cu–N(axial ligand)=2.17 Å.[17]

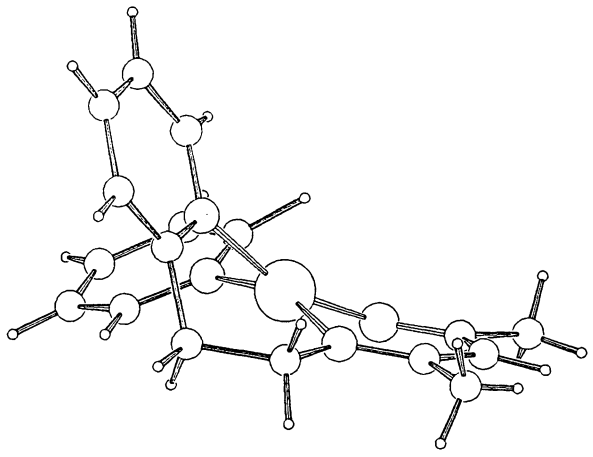

Fig. 4. Edge-on view of $[Cu(L^2)(py)]ClO_4$ showing a tetrahedral distortion.

**Magnetic Susceptibilities.** The magnetic behaviors of **1** and **3** are shown in Figs. 5 and 6, respectively, in the forms of the $\chi_A$ vs. $T$ and $\mu_{eff}$ vs. $T$ plots, where $\chi_A$ is the magnetic susceptibility per copper, $\mu_{eff}$ the effective magnetic moment per copper, and $T$ the absolute temperature. The numerical data of the magnetic susceptibilities of **1**, **2**, and **3** are given as supplementary data. Essentially similar magnetic behaviors were observed for **1** and **2**, hence are exemplified by that of **1**. The $\mu_{eff}$ of **1** is 1.69 $\mu_B$ at 290 K which is slightly smaller

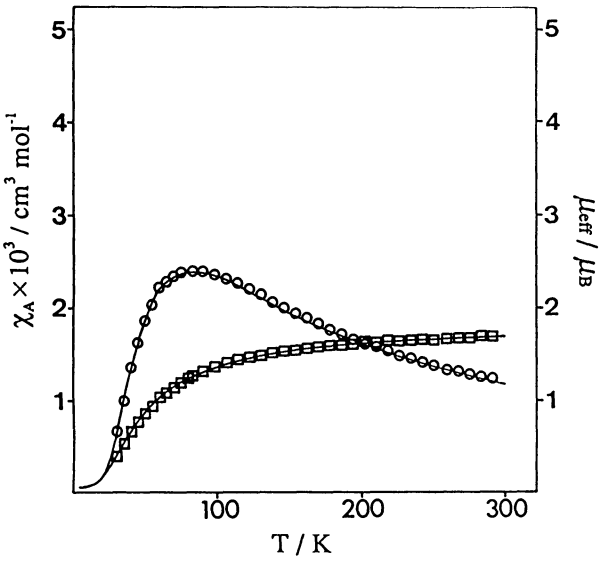


Fig. 5. Temperature dependences of the magnetic susceptibility per copper $\chi_A$(○) and the effective magnetic moment ef $\mu_{eff}$(□) for **1**.

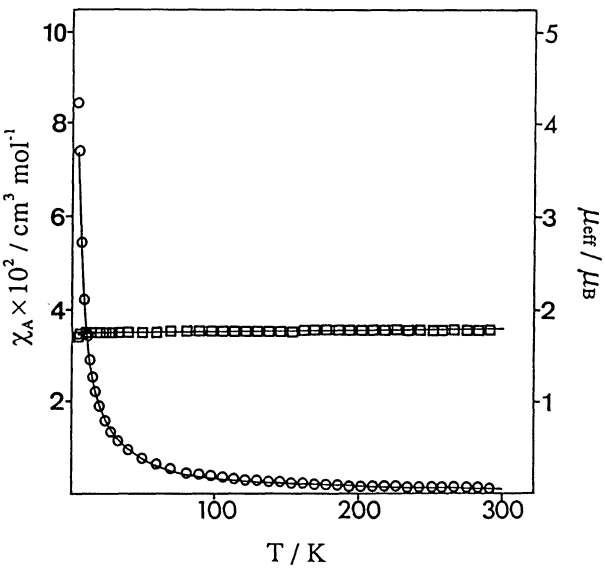


Fig. 6. Temperature dependences of the magnetic susceptibility per copperx $\chi_A$(○) and the effective magnetic moment $\mu_{eff}$(□) for **3**.

than the spin-only value 1.73 $\mu_B$ of $S=1/2$. As the temperature is lowered, the $\mu_{eff}$ value decreases gradually from 1.69 $\mu_B$ at 290 K to 0.4 $\mu_B$ at 30 K, indicating an antiferromagnetic spin-coupling between Cu(II) ions through the imidazolate group. The $\chi_A$ vs. $T$ curve showed a maximum at 80 K, which is one of the characteristic features of binuclear copper(II) complexes exhibiting intramolecular antiferromagnetic spin-coupling. The magnetic susceptibility data were interpreted quantitatively by the Bleaney-Bowers equation (1) derived from the spin Hamiltonian $H=-2JS_{Cu}\cdot S_{Cu}$

$$\chi_A = Ng^2\beta^2/kT(3+\exp(-2J/kT)) + N\alpha \quad (1)$$

In the equation (1), the symbols have their usual meanings. The observed susceptibility data were fitted by least-squares method, where the disagreement factor $R=\sum[(\chi(obsd)-\chi(calcd))^2/\sum\chi(obsd)^2]^{1/2}$ was minimized and the temperature independent paramagnetizm term was taken as $N\alpha=60\times10^{-6}$ mol$^{-1}$cm$^3$. The best-fit parameters $J=-46.1$ cm$^{-1}$, $g=2.03$, and $R=8.76\times10^{-5}$ were obtained, and the theoretical $\chi_A$ and $\mu_{eff}$ curves with the fitting parameters are shown by solid lines in Fig. 5. The same procedure was applied to **2** and the best-fit parameters of $J=-36.6$ cm$^{-1}$, $g=2.02$, and $R=6.35\times10^{-4}$ were obtained.

The $\chi_A$ curve of **3** increases smoothly as the temperature is lowered, showing no maxima in the temperature range studied. The $1/\chi_A$ vs. $T$ curve obeys the Curie-law. The $\mu_{eff}$ is temperature independent and the value 1.79 $\mu_B$ is close to the spin-only value 1.73 $\mu_B$ of $S=1/2$. These facts demonstrate that the Cu(II)-Cu(II) magnetic interaction of **3** is undetectable in the temperature range studied.

ESR spectra of the reference complexes [Cu(L$^n$)(*N*-MeIm)]ClO$_4$ showed an axial pattern and the $g$ values are obtained. [Cu(L$^1$)(*N*-MeIm)]ClO$_4$: $g_\perp=2.06$, $g_{//}=2.17$; [Cu(L$^2$)(*N*-MeIm)]ClO$_4$: $g_\perp=2.06$, $g_{//}=2.15$; [Cu(L$^3$)(*N*-MeIm)]ClO$_4$: $g_\perp=2.06$, $g_{//}=2.18$. On the basis of the ESR spectra, the unpaired electron of [Cu(A)] and [Cu(L$^n$)(*N*-MeIm)]ClO$_4$ ($n$=1, 2, 3) occupies the $d_{x^2-y^2}$ orbital lying in their basal coordination planes.[18] When imidazolate moiety bridges two copper(II) ions at their equatrial sites, the $\sigma$-$\sigma$ super-exchange through imidazolate moiety is possible to produce antiferromagnetic spin-coupling between copper(II) ions. Thus, the antiferromagnetic interaction of **1** and **2** can be explained by the $\sigma$-$\sigma$ superexchange mechanism, although large deviation from the coplanarity of two coordination planes is estimated on the basis of the crystal structures of the reference complexes. The antiferromagnetic spin-coupling constants $-J$ for **1** ($J=-46.1$ cm$^{-1}$) and **2** ($J=-36.6$ cm$^{-1}$) are in the range reported for imidazolate-bridged copper(II) complexes.[9,19] The values are smaller than those of [Cu(A)-Cu(tfac)$_2$] ($J=-56$ cm$^{-1}$, tfac=trifluoroacetylacetonate) and [Cu(A)Cu(tebima)]$^{2+}$ ($J=-70$ cm$^{-1}$, tebima=tris[(1-ethyl-1*H*-benzimidazol-2-yl)methyl]amine),[9] probably due to a large deviation from coplanarity. On the other hand, $\sigma$-$\sigma$ superexchange is not possible for **3**, becuase the unpaired electron of [Cu(L$^3$)] moiety occupies the d orbital lying in the equatorial plane which is perpendicular to [Cu(A)] moiety.

This work was in part supported by a Grant-in-Aid for Scientific Research No. 01540515 from the Ministry of Education, Science and Culture.

## References

1) O. Kahn, *Struct. Bonding (Berlin)*, **68**, 89 (1987).
2) C. J. Carins and D. H. Busch, *Coord. Chem. Rev.*, **69**, 1 (1986).
3) N. Matsumoto, K. Inoue, H. Ōkawa, and S. Kida, *Chem. Lett.*, **1989**, 1079.
4) Z. J. Zhong, H. Ōkawa, N. Matsumoto, H. Sakiyama, and S. Kida, *J. Chem. Soc., Dalton Trans.*, **1991**, 497.
5) Z. J. Zhong, N. Matsumoto, H. Ōkawa, and S. Kida, *Inorg. Chem.*, **30**, 436 (1991).
6) N. Matsumoto, M. Sakamoto, H. Tamaki, H. Ōkawa, and S. Kida, *Chem. Lett.*, **1990**, 853.
7) H. Ōkawa and S. Kida, *Inorg. Chim. Acta*, **23**, 253 (1977).
8) E. Sinn and C. M. Harris, *Coord. Chem. Rev.*, **4**, 391 (1969).
9) N. Matsumoto, T. Akui, H. Murakami, J. Kanesaka, A. Ohyoshi, and H. Ōkawa, *J. Chem. Soc., Dalton Trans.*, **1988**, 1021.
10) N. Matsumoto, H. Murakami, T. Akui, J. Honbo, H. Ōkawa, and A. Ohyoshi, *Bull. Chem. Soc. Jpn.*, **59**, 1609 (1986).
11) J-P. Costes, F. Dahan, and J-P. Laurent, *Inorg. Chem.*, **30**, 1887 (1991), and references therein.
12) L. Sacconi and I. Bertini, *Inorg. Chem.*, **5**, 1520 (1966).
13) R. R. Gagne, *J. Am. Chem. Soc.*, **98**, 6709 (1976).
14) E. A. Boudreaux and L. N. Mulay, "Theory and Application of Molecular Paramagnetism," Wiley, New York (1976), pp. 491—495.
15) "Internationaol Tables for X-Ray Crystallography," Kynoch Press, Burmingham (1974), Vol. 4.
16) T. Sakurai and K. Kobayashi, *Rikagaku Kenkyusho Houkoku*, **55**, 69 (1979); S. Kawano, *Rep. Comput. Cent., Kyushu University*, **13**, 39 (1980).
17) O. P. Anderson and A. B. Packard, *Inorg. Chem.*, **19**, 2123 (1980); M. J. Maroney and N. J. Rose, *Inorg. Chem.*, **23**, 2252 (1984).
18) Y. Nishida and S. Kida, *Coord. Chem. Rev.*, **27**, 275 (1979).
19) J. P. Costes and M. I. F-Garcia, *Inorg. Chim. Acta*, **173**, 247 (1990).